Chemical Science

ROYAL SOCIETY OF CHEMISTRY

EDGE ARTICLE

View Article Online
View Journal | View Issue

Cite this: *Chem. Sci.*, 2021, **12**, 2674

All publication charges for this article have been paid for by the Royal Society of Chemistry

Photo-modulated wide-spectrum chromism in Eu^{3+} and Eu^{3+}/Tb^{3+} photochromic coordination polymer gels: application in decoding secret information†

Parul Verma, Ashish Singh and Tapas Kumar Maji *

Photo-switching emission of photochromic materials has paramount importance in the field of optoelectronics. Here, we report synthesis and characterization of a dithienylethene (DTE) based photochromic low molecular weight gelator (LMWG) and self-assembly with lanthanide (Eu^{3+} and Tb^{3+}) ions to form a photochromic coordination polymer gel (pcCPG). Based on DTE ring opening and closing, the TPY-DTE gel shuttles from pale-yellow coloured TPY-DTE-O to dark blue coloured TPY-DTE-C and *vice versa* upon irradiating with UV and visible light, respectively, and both the photoisomers show distinct optical properties. Furthermore, integration of Eu^{3+} and Tb^{3+} lanthanides with TPY-DTE resulted in red and green emissive Eu-pcCPG (Q.Y. = 18.7% for the open state) and Tb-pcCPG (Q.Y. = 23.4% for the open state), respectively. The photoisomers of Eu-pcCPG exhibit photo-switchable spherical to fibrous reversible morphology transformation. Importantly, an excellent spectral overlap of the Eu^{3+} centred emission and absorption of DTE in the closed form offered photo-switchable emission properties in Eu-pcCPG based on pcFRET (energy transfer efficiency >94%). Further, owing to the high processability and photo-switchable emission, the Eu-pcCPG has been utilized as invisible security ink for protecting confidential information. Interestingly, mixed Eu^{3+}/Tb^{3+} pcCPG exhibited photo-modulated multi-spectrum chromism reversibly where the colour changes from yellow, blue, and red to green and *vice versa* under suitable light irradiation.

Received 16th October 2020
Accepted 21st December 2020

DOI: 10.1039/d0sc05721e

rsc.li/chemical-science

Introduction

The recent upsurge in research on coordination polymer gels (CPGs),[1–3] a new class of processable 'soft' materials formed by the self-assembly of suitable metal ions and a low molecular weight gelator (LMWG),[4] stems from their unique properties including responsiveness to stimuli,[5] environmental adaptation,[6] tunable degradability,[7] self-healing,[8] and dynamic nanoscale architecture.[9] The synergistic interactions between metal ions and LMWGs offer unique properties for CPGs in the optical,[10] magnetic,[11] redox,[12] and catalysis fields.[13] Lanthanide-based coordination compounds[14] with a π-chromophoric ligand show greater superiority as light-emitting materials due to their large Stokes shifted narrow visible/near infra-red (NIR) emission with a long excited-state lifetime.[15,16] Recently, the integration of lanthanide ions, in particular Eu^{3+}, with suitable photochromic organic molecules has received considerable attention as their photo-responsive tunable emission[17] based on pcFRET (photochromic Förster resonance energy transfer) has led to applications in optical switches,[18–22] data storage, super-resolution imaging,[23] molecular machines,[24,25] sensing[26–29] and optoelectronic devices.[30] Among the different photochromes, dithienylethene (DTE) or diarylethene (DAE) derivatives are widely studied[31–35] because of their outstanding fatigue resistance,[36] high photoisomerization quantum yield,[37–39] and easy synthesis with different functional groups.[40–42] Moreover, light is an intriguing external stimulus as it offers clean and noninvasive control[35] of the operation with high accuracy, showing greater convenience in activating or erasing the secret encoded information as compared to other chemical stimuli.[23] Therefore, for reversible information encryption and decryption, it is desirable to develop soft processable photo-switchable luminescent nanomaterials which are capable of being easily operated in a noninvasive manner.[13] Furthermore, light stimulus driven reversible dynamic transformation of the morphology in such soft nano materials is of paramount importance in the field of opto-electronics, drug delivery[43,44] and photo actuators.[45] The Eu^{3+} integrated photochromic materials wherein the light can change the optical signal output[46] would be ideal candidates bearing extra security features of non-tampering, anti-counterfeiting[47] or forgery of encoded information.[48,49] Thus,

Molecular Material Laboratory, Chemistry and Physics of Material Unit, School of Advanced Materials (SAMat), Jawaharlal Nehru Centre for Advanced Scientific Research, Jakkur, Bangalore-560064, India. E-mail: tmaji@jncasr.ac.in

† Electronic supplementary information (ESI) available. See DOI: 10.1039/d0sc05721e

they can be utilized as secret ink[50] for storing confidential information and could be useful for intelligence agencies, defense authorities, and private or government security organizations. However, photo-modulated emission of Eu^{3+} is mainly studied in the solid-state,[48,49,51,52] and therefore, processability will be the main obstacle for using them as security ink.[53] We envisioned that the design and synthesis of such lanthanide integrated photochromic (Ln-pcCPG) soft materials would show greater processability[54,55] and high thermal stability due to metal coordination.[56,57] Compared to single-colour emissive materials, bi-metallic lanthanide (Eu^{3+}/Tb^{3+}) CPGs with a photochromic LWMG would offer the potential for more sensitive stimuli-responsive multi-colour properties.[58] The colour of the mixed (Eu^{3+}/Tb^{3+}) CPG can be readily modulated over a wide spectrum by light stimulus and can be used for multi-colour signaling and sensing purposes.[59] Such soft processable multi-spectrum chromism based on mixed lanthanide emissive pcCPGs is underexplored (Scheme 1).[54]

Here, we report the design and synthesis of a photochromic LMWG based linker (TPY-DTE) by integrating the DTE unit and terpyridine moiety through an amide linkage. TPY-DTE LMWG showed excellent photochromism in the gel state. Furthermore, two photochromic CPGs, Eu-pcCPG and Tb-pcCPG, were prepared by the self-assembly of Eu^{3+} and Tb^{3+} salts with TPY-DTE LMWG, respectively. A reversible morphological transformation between the microspheres and fibers was also demonstrated in the Eu-pcCPG along with the photochromic behaviour. Interestingly, Eu-pcCPG displayed fast photo-switchable emission properties based on a highly efficient pcFRET process (energy transfer efficiency = 94.79%). Further, highly processable photo-switchable emission Eu-pcCPG has been used as invisible security ink on ordinary paper and also exploited for decoding of confidential information. On the other hand, Tb-pcCPG did not exhibit photo-switchable emission; however, an optimized pcCPG of mixed metal Eu^{3+} : Tb^{3+} (7 : 3 ratio) has shown interesting photo-modulated reversible emission as well as visible colour changes that can be employed for signalling and sensing applications.

Results and discussion

Synthesis, characterization, and applications of photochromism in organogels

Synthesis and characterization of the photochromic molecule, 4,4′-(perfluorocyclopent-1-ene-1,2-diyl)-bis-(5-methylthiophene-2-carboxylic acid) ($DTE(COOH)_2$), has been reported in the literature.[60] We have adopted a similar synthetic procedure, and the details are given in the ESI (Scheme S1†). The photochromic low molecular weight gelator (LMWG), namely 4,4′-(perfluorocyclopent-1-ene-1,2-diyl)bis(*N*-(3-([2,2′ : 6′,2″-terpyridin]-4′-ylamino)propyl)-5-methylthiophene-2-carboxamide) (TPY-DTE), was synthesized by amide coupling between the $DTE(COOH)_2$ photochrome and 2,2′ : 6′,2″-terpyridin-4′-yl-propane-1,3-diamine ($TPY\text{-}NH_2$) and characterized using different spectroscopic techniques (Fig. S1–S3†). UV-Vis absorption study for a methanolic solution (10^{-5} M) of yellow coloured TPY-DTE showed an overlap band in the range of 264–286 nm, which is attributed to π-π* transition for TPY[30] and $DTE(COOH)_2$ units[60](Fig. S4†). Upon irradiation with UV light (λ = 365 nm) for 15 seconds, the yellow colour solution changes to

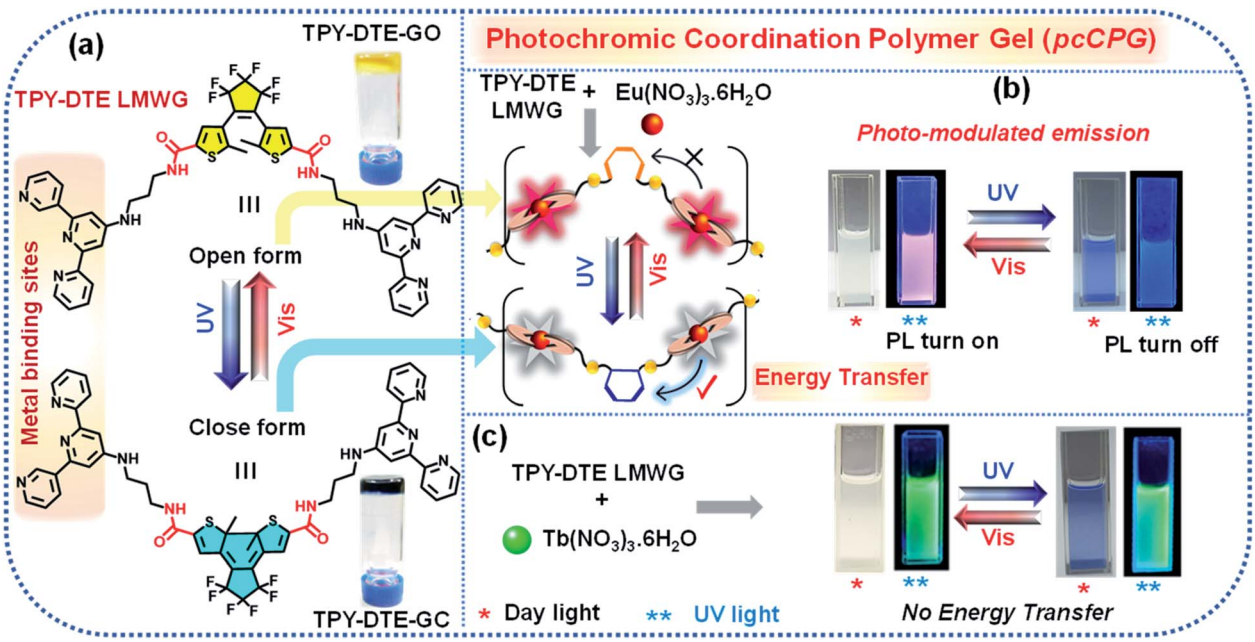

Scheme 1 (a) Photoisomerization in TPY-DTE LMWG and the corresponding visible colour changes in the TPY-DTE organogel. (b) Schematic representation of the Eu^{3+} coordinated TPY-DTE LMWG in Eu-pcCPG (open and closed form) and the corresponding images of the xerogel in the dispersed state showing photomodulated colour changes under daylight/UV light. (c) Images of the Tb-pcCPG xerogel in the dispersed state under daylight/UV light.

blue because of the ring-closing of the DTE unit.[54] The presence of additional absorbance between 500–700 nm in the UV-Vis absorption spectrum after UV irradiation further confirms the photocyclization of the DTE units in the LMWG (Fig. S4a†).[5] Notably, saturation of DTE-ring closing was observed upon UV irradiation for ~60 s (Fig. S4a†). Further, the photocycloreversion (DTE ring-opening) in TPY-DTE LMWG was observed upon visible light irradiation (λ > 400 nm), and completion of the reaction was achieved in ~110 s (Fig. S4b†). The quantum efficiency for the conversion of the open to the closed form (TPY-DTE) and *vice versa* was calculated to be 81% and 69%, respectively (Fig. S4c and d†).[37,38] Moreover, the maximum conversion of the open to the closed form in the photostationary state (PSS) upon UV-light irradiation was found to be ~72%. The gelation propensity of LMWG was examined in various solvent systems under different conditions (Table S1, see the ESI† for details). For organogel (OG) preparation, the LMWG (5 mg) was taken in a 0.3 mL solvent mixture of methanol (0.2 mL), ethylene glycol (0.05 mL) and water (0.05 mL). The reaction mixture was heated gradually from 60 °C to 120 °C in a closed vial and subsequently cooled to room temperature which resulted in a pale yellow coloured organogel (OG) of TPY-DTE (Fig. 1a and S5–S7†). The gel can be converted to the sol form by heating at 80 °C, confirming the thixotropic behaviour (Fig. S7†). The yellow gel (TPY-DTE-GO *i.e.* gel in the open form) can be converted to the dark blue coloured gel (TPY-DTE-GC *i.e.* gel in the closed form) upon irradiating with UV-light for 10–15 seconds and can be reverted to yellow colour by treating with visible light for 25–30 seconds (Fig. 1a). The UV-Vis absorption spectra of TPY-DTE-GO also showed the overlap bands in the range of 264 nm to 290 nm, which are characteristic of the π–π^* transition for both, TPY and DTE units (Fig. 1d). On the other hand, TPY-DTE-GC showed additional broad absorbance in the visible region with a maximum at 610 nm due to the ring closing of the DTE unit. The reversibility of photochromic behaviour of the TPY-DTE gel has been examined for ten cycles and found to be equally effective as for the 1st cycle, suggesting excellent fatigue resistance behaviour of the gel (Fig. 1d and S8a†). Similar to the TPY-DTE LMWG, upon continuous UV-light irradiation on the TPY-DTE-GO, UV-Vis absorption spectra were recorded in a time interval of three seconds, and the maximum conversion from TPY-DTE-GO to TPY-DTE-GC can be achieved in ~60 seconds (Fig. S8b†).

Similarly, the complete reversible conversion of TPY-DTE-GC to TPY-DTE-GO can be achieved in ~120 seconds with continuous visible light irradiation as confirmed by the UV-Vis absorption spectrum (Fig. S8c†). The reversible fast-photochromism in the TPY-DTE organogel as compared to previously reported DTE-based solid photochromic materials[49,61] could be attributed to its gelacious nature, which provides more space for facile structural changes during the photo reaction.[54] The powder X-ray diffraction (PXRD) pattern of the TPY-DTE-GO showed a peak at $2\theta = 26.43°$, corresponding to a d-spacing value of 3.36 Å which indicates the presence of π–π stacking in the self-assembly (Fig. S6†). Comparison of the FTIR spectra of TPY-DTE LWMG and the TPY-DTE-OG revealed a decrease in –C=O and –N–H stretching frequencies from 1696 cm^{-1} to 1684 cm^{-1} and from 3462 cm^{-1} to 3436 cm^{-1}, respectively, indicating the presence of intermolecular H-bonding between the amide groups of DTE-TPY (Fig. S5†).[62] The surface morphology of TPY-DTE-GO and TPY-DTE-GC was analyzed by FE-SEM (Fig. S9†). This showed irregular interconnected sheet-like morphologies for both cases, ensuring that the supramolecular architecture remains unaffected by the light treatment. This was further supported by the high-resolution TEM (HR-TEM) analysis as similar layered sheet

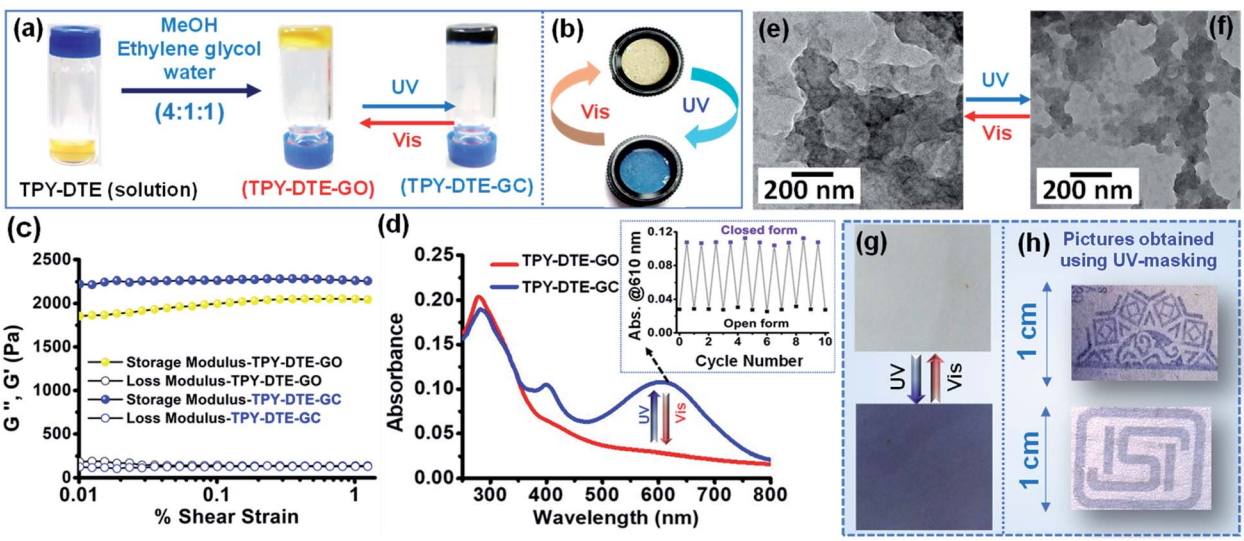

Fig. 1 (a) Preparation of the TPY-DTE organogel and photoisomerization of TPY-DTE-GO to TPY-DTE-GC and *vice versa*. (b) Photochromism in TPY-DTE in the xerogel state. (c) Strain sweep tests for TPY-DTE-GO and TPY-DTE-GC at $\gamma\% = 0.01$–1. (d) Absorption spectra for TPY-DTE-GO and TPY-DTE-GC (the inset shows the recyclability test for 10 consecutive cycles) (absorbance changes at 610 nm for the TPY-DTE organogel upon visible and UV-light treatment). HR-TEM images for (e) TPY-DTE-GO and (f) TPY-DTE-GC. (g) Coating of an ethanolic solution of TPY-DTE-GO on white paper and the corresponding photochromism. (h) Various patterns obtained by masking on TPY-DTE organogel-coated paper.

type morphology was observed for both the photo-isomers (Fig. 1e and f). The rheology measurements for TPY-DTE-GO and TPY-DTE-GC showed that the storage modulus G' was considerably higher than the loss modulus G'' for both, indicating the elastic properties of the self-assembly, which is characteristic of a stable gel phase[54] (Fig. 1c). Notably, an increase in the G' value was observed for TPY-DTE-GC as compared to TPY-DTE-GO, which could be attributed to the greater mechanical strength due to stronger π–π stacking in the planar configuration of the closed-ring photoisomer.[63] The photoconversion of TPY-DTE-GO to TPY-DTE-GC was further confirmed through IR spectra which showed a characteristic shift of CH_3 bending linked to thiophene rings from 985 cm^{-1} to 996 cm^{-1} for open to closed form conversion (Fig. S5†).[64,65] The quantum efficiency for the conversion of TPY-DTE-GO to TPY-DTE-GC and *vice versa* was calculated to be 60% and 46%, respectively (Fig. S10†).[37] Moreover, the maximum conversion of TPY-DTE-GO to TPY-DTE-GC in the photostationary state (PSS) upon UV-light irradiation was found to be ~71%. Owing to the excellent processability, we have exploited yellow coloured TPY-DTE-GO for writing applications by coating over an ordinary paper (Fig. 1g). The light-yellow gel-coated paper turned blue in colour upon UV-irradiation for ~15 seconds and reverted to a light-yellow colour upon shining visible light for ~30 seconds. Further, various designs have been made just in a few seconds upon UV-light irradiation through UV-masking, indicating the potential of the material to be used in the lithographic technique, ordinary UV-sensors, and writing applications[37,55] (Fig. 1h).

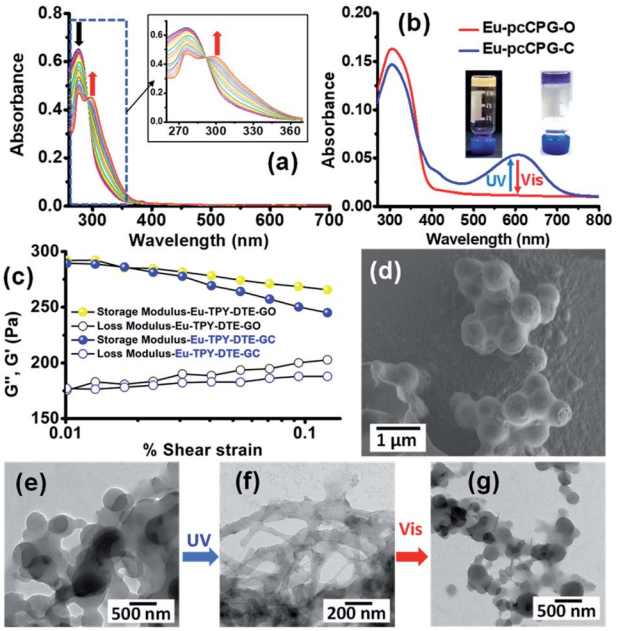

Fig. 2 (a) Titration of TPY-DTE LMWG with Eu^{3+} in methanol (inset: from 270 nm to 360 nm). (b) Absorption spectra of Eu-pcCPG-O (yellow gel) and Eu-pcCPG-C (blue gel) and the corresponding images under daylight. (c) Strain sweep tests for Eu-pcCPG-O and Eu-pcCPG-C at $\gamma\% = 0.01$–0.1. (d) FESEM and (e) TEM images of Eu-pcCPG-O. (f) TEM images of Eu-pcCPG-C (obtained by UV irradiation on Eu-pcCPG-O). (g) TEM images of Eu-pcCPG-O (obtained by visible light irradiation on Eu-pcCPG-C).

Synthesis, characterization, and photochromism in coordination polymer gels

We envisioned utilizing TPY-DTE LMWG as a linker for preparing a photochromic coordination polymer gel (pcCPG) by integrating with a suitable metal ion. In this context, we have chosen lanthanide metal ions (Eu^{3+} and Tb^{3+}) for preparing pcCPG as they form complexes with TPY units which exhibit narrow emission with an excellent quantum yield and also possess a long excited-state lifetime.[53] The UV-Vis absorption spectra obtained from titration of Eu^{3+} (stock solution = 10^{-4} M) with TPY-DTE LMWG (10^{-6} M) in methanol have suggested a maximum binding ratio of 1 : 1 (Fig. 2a) and showed the bathochromic shift of TPY absorption from 276 nm to 300 nm due to metal binding.[66] The binding constant (K_a) for Eu^{3+} to TPY-DTE LMWG was calculated using the Benesi–Hildebrand plot[67] and found to be 4.54×10^4 M^{-1} (Fig. S11†). Next, gelation was attempted with an equimolar ratio of Eu^{3+} and TPY-DTE under similar conditions as employed for TPY-DTE OG and resulted in the yellow coloured Eu-pcCPG-O (gel in the open form) (Fig. 2b and S12–S14†). FE-SEM and TEM analysis of Eu-pcCPG-O showed a nano-sized (300–600 nm) interconnected spherical morphology (Fig. 2d and e). EDAX analysis indicated the presence of 11.84 wt% Eu^{3+} in Eu-pcCPG-O, which is in good agreement with the theoretical prediction (Fig. S14a†). Elemental mapping demonstrated the uniform distribution of Eu^{3+} in the supramolecular network (Fig. S14b†). The PXRD pattern of Eu-pcCPG-O showed a low angle peak at 7.68° (d = 11.5 Å), indicating the formation of a higher-order self-assembled structure upon Eu^{3+} coordination to the TPY centre (Fig. S13†). Notably, PXRD peaks at $2\theta = 24.53°$ ($d = 3.6$ Å) and 26.25° ($d = 3.4$ Å) indicated the presence of π–π stacking in the self-assembly in Eu-pcCPG-O (Fig. S13†). Further, FT-IR analysis revealed a significant shift in the C=O stretching frequency of Eu-pcCPG-O ($\nu = 1642$ cm^{-1}) in comparison to the TPY-DTE-GO ($\nu = 1684$ cm^{-1}) that can be attributed to the stronger H-bonding (*i.e.* C=O···H–N– interactions) in Eu-pcCPG-O which is also supported by the appearance of an intense peak at 3455 cm^{-1} for ν(N–H) (Fig. S12†). The UV-Vis absorption spectrum of the yellow Eu-pcCPG-O showed a subtle bathochromic shift as compared to that of TPY-DTE-GO and the absorption maximum was found to be at 310 nm. Next, irradiation of yellow coloured Eu-TPY-DTE-O pcCPG with UV-light for 30 seconds resulted in deep blue colouration due to the DTE ring-closing and confirmed the formation of the photo isomer Eu-pcCPG-C (gel in the closed form) (Fig. 2b). Eu-pcCPG-C revealed broad absorption in the visible range (500–750 nm) similar to TPY-DTE-GC (Fig. 2b). Importantly, visible light irradiation for 60 seconds caused blue Eu-pcCPG-C to further revert to yellow Eu-pcCPG-O. The UV-Vis absorption properties were examined back and forth from yellow (Eu-pcCPG-O) to blue (Eu-pcCPG-C) and *vice versa* upon irradiation with UV and visible light, respectively, for ten cycles and were found to be equally efficient as observed for the first cycle (Fig. S15†). The quantum

efficiencies for the conversion of Eu-pcCPG-O to Eu-pcCPG-C and *vice versa* in the gel state were found to be 70% and 57%, respectively (Fig. S16†). The conversion ratio of Eu-pcCPG-O to Eu-pcCPG-C in the photostationary state (PSS) was calculated to be ~71%. Next, the morphology of Eu-pcCPG was studied by TEM analysis with UV and visible light irradiation (Fig. 2e and f). Interestingly, upon UV light irradiation on the Eu-pcCPG-O for 2 min, the aggregated nanospheres were transformed into interconnected nanofibrous structures due to DTE ring-closing (Fig. 2f). Further, the reversibility of the morphology was investigated by visible light irradiation on the Eu-pcCPG-C. The regaining of the nano spherical morphology was achieved upon visible light irradiation for 10 min (Fig. 2g). This exclusive photoinduced reversible morphology transformation from spheres to fibers could enable the use of such materials in the domains of photoactuators[4,39] and delivery media.[45,68] Next, a rheology study was performed for Eu-pcCPG-O and Eu-pcCPG-C, which showed the viscoelastic nature of both the photo-isomers of pcCPG. Notably, G' for both Eu-pcCPG-O and Eu-pcCPG-C was found to be similar under less % strain, which decreases along with an increase in the % strain. The decrease is more pronounced from 0.02% to 0.1% strain for Eu-pcCPG-C which suggested the lower mechanical strength of the Eu-pcCPG-C as compared to Eu-pcCPG-O (Fig. 2c). Next, upon excitation at 310 nm, the Eu-pcCPG-O exhibited Eu^{3+} centred red emission at 590 ($^5D_0$–$^7F_1$), 615 ($^5D_0$–$^7F_2$), 652 ($^5D_0$–$^7F_3$), and 700 ($^5D_0$–$^7F_4$) nm[54] (Fig. 3a). This can be easily discerned by the naked eye. Interestingly, the highest intensity emission peak of Eu^{3+} at 615 nm has excellent overlap with the absorption of Eu-pcCPG-C; thus, reversible photo-switchable luminescence of Eu-pcCPG can be realized based on a pcFRET process (Fig. 3a). The emission of Eu-pcCPG-O was almost quenched upon continuous UV irradiation for 70 s (Fig. 3b–e), which can be attributed to the formation of Eu-pcCPG-C. Furthermore, visible light irradiation on the blue-coloured Eu-pcCPG-C for 300 seconds revealed the reversion to yellow coloured Eu-pcCPG-O along with complete recovery of the corresponding Eu^{3+} based red emission (Fig. 3c and f). The DTE-ring opening was further confirmed by the absence of the absorption band in the range of 500–750 nm in the UV-Vis absorption spectrum of the obtained yellow Eu-pcCPG-O (Fig. 2b). The absolute quantum yields for Eu-pcCPG-O and its photo-isomer, Eu-pcCPG-C, were found to be 18.7% and 0.52%, respectively. Next, the rate constant has also been calculated for quenching and regaining of fluorescence by irradiating Eu-pcCPG (Fig. 3e and f). The change in the emission intensity was monitored at 615 nm, and the rate constant for fluorescence quenching and regaining was calculated to be 5.89×10^{-2} s^{-1} and 9.09×10^{-3} s^{-1}, respectively (Fig. 3e and f). The rate constant study showed that DTE ring-opening takes a longer time as compared to ring-closing in Eu-pcCPG. Further, excited-state lifetimes were measured for Eu-pcCPG-O and its photo-irradiated form, Eu-pcCPG-C, upon excitation at 310 nm (Fig. 3g). The data of the lifetime for Eu-pcCPG-O and Eu-pcCPG-C were fitted using bi-exponential decay,[69] indicating the presence of two distinct emitting centres which are most likely to appear due to two different coordination environments around the Eu^{3+} centre in the Eu-pcCPG. The Eu^{3+} centre in Eu-pcCPG carries two terpyridine

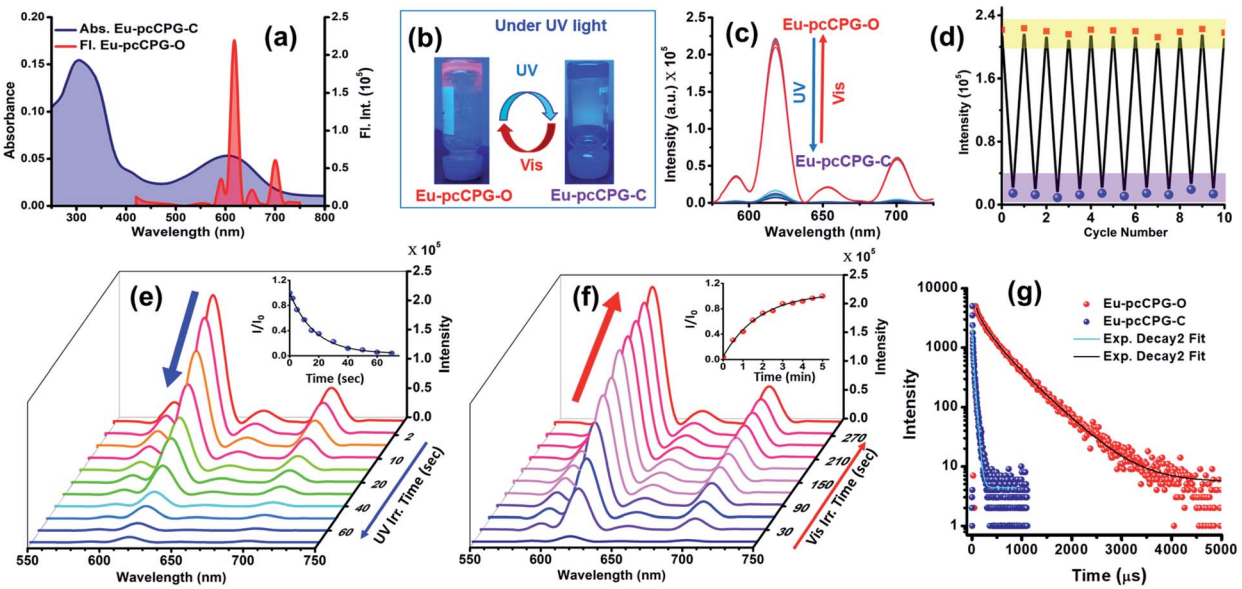

Fig. 3 (a) The absorption of Eu-pcCPG-C (blue) and emission for Eu-pcCPG-O (red). (b) The images for Eu-pcCPG-O (showing red emission) and Eu-pcCPG-C (showing no emission) under UV light. (c) Emission spectrum for the Eu-pcCPG-O and Eu-pcCPG-C upto 10 consecutive cycles for emission regaining and quenching upon visible and UV light irradiation, respectively. (d) Corresponding change in emission intensity at 615 nm for 10 cycles. (e) Time dependent change in the emission for Eu-pcCPG-O upon UV light irradiation (inset: kinetics plot for emission quenching upon UV light irradiation). (f) Time dependent change in the emission for Eu-pcCPG-C upon visible light irradiation (inset: the kinetics plot of emission regaining upon visible light irradiation). (g) Time resolved photoluminescence decay profiles for Eu-pcCPG-O and Eu-pcCPG-C (λ_{ex} = 310 nm and λ_{em} = 615 nm).

units (occupying six coordination sites) and the remaining two coordination sites could be occupied by the water or nitrate anions or both (one water and one nitrate anion),[70,71] which leads to the Eu^{3+} centres in two different coordination environments. This would change the ligand field strength around the Eu^{3+} centre in Eu-pcCPG that eventually results in the biexponential decay. The average lifetimes for Eu-pcCPG-O and Eu-pcCPG-C were calculated to be 397.0 μs and 20.7 μs, respectively (see the ESI for details and Table S2†). The significantly decreased excited-state lifetime of Eu-pcCPG-C provided strong support for the pcFRET process. The energy transfer efficiency calculated from the excited-state lifetime was found to be 94.79% (see the details in the ESI†). This further validated the existence of strong pcFRET in the Eu-pcCPG.

Secret writing application

The Eu-pcCPG exhibited excellent processability, photochromism, and photo-switchable emission. Therefore, we envisioned utilizing this as an invisible security ink. For this purpose, an ink based on the light-yellow methanolic solution of Eu-pcCPG-O was prepared (Fig. 4a). A message was written on a yellow coloured ordinary paper, which was unreadable due to the paper having a similar background colour (Fig. S16†). At the same time, it became red emissive and could be read out easily under UV-light. Notably, upon exposure to UV light for ~45 seconds, the red emission was quenched, and the written information turned to blue colour which could be read out easily by the naked eye, thus failing to hide the information (Fig. S17†). To overcome this issue, we used a blue paper, which had negligible auto-emission, for encoding the information (Fig. 4a). We coated Eu-pcCPG-O on the blue paper which was not visible by the naked eye under ambient light. However, it showed Eu^{3+} based red emission under UV light (Fig. 4b). Next, we utilized a barcode pattern as the UV-mask, which was created for our institute (JNCASR). UV-light was irradiated for 45 seconds upon employing the barcode-based UV-mask over the Eu-pcCPG-O coated area. This resulted in fluorescence quenching along with turning the colour to blue in the mask free area, which is interestingly invisible due to having a similar background colour to the paper (Fig. 4c). At the same time, a barcode pattern was generated, which was red-emissive and visible only under UV light (Fig. 4d). Importantly, this barcode pattern disappeared upon continuous UV-irradiation for ~45 seconds (Fig. 4e). Nevertheless, the time was found to be sufficient for scanning the information using an ordinary mobile phone scanner (Fig. 4f) (see Video VS1†). This demonstrates the writing application of Eu-pcCPG for fast reading and erasing capability and showed potential for utilization for security purposes.[50]

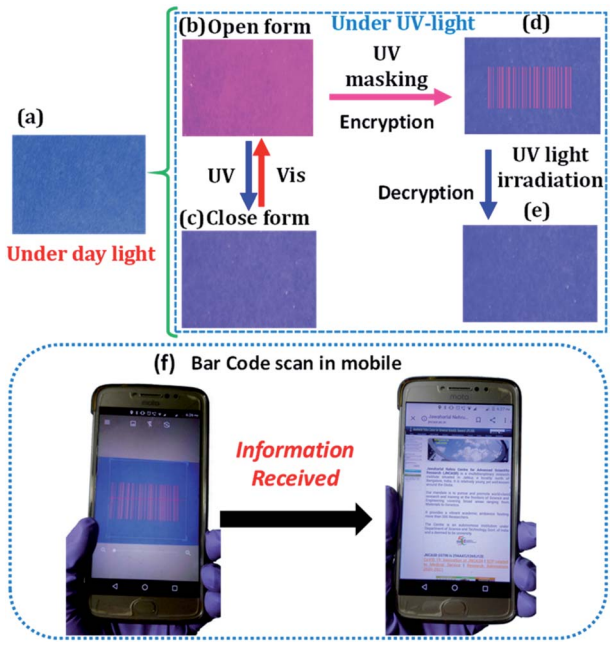

Fig. 4 Encryption/decryption application: (a) the methanolic solution of Eu-pcCPG-O (2 mg in 1 mL methanol) coated on a normal blue paper. (b) Blue paper turning red under UV light due to Eu-pcCPG-O emission. (c) Red emissive paper turns blue after UV-irradiation due to formation of Eu-pcCPG-C. (d) Printing of a barcode using a UV mask, *i.e.* encryption of the pattern. (e) Decryption of the pattern upon UV light irradiation for 45 seconds. (f) Barcode scanning using a mobile phone.

Terbium based pcCPG and mixed Tb^{3+} & Eu^{3+} based pcCPG for wide-spectrum chromism

The titration of Tb^{3+} (stock solution = 10^{-4} M) was performed in the methanolic solution of TPY-DTE LMWG (10^{-6} M) and the corresponding UV-Vis spectra suggested a binding ratio of 1 : 1 for Tb^{3+} with LMWG (Fig. S18a†). Similar to Eu-pcCPG, the binding constant (K_a) for Tb^{3+} to TPY-DTE LMWG was determined and found to be 5.05×10^4 M^{-1} (Fig. S18b†). The Tb^{3+} coordinated pcCPG gel (Tb-pcCPG) was prepared and characterized by adopting similar procedures and techniques as employed for Eu-pcCPG (see the details in the ESI†). Tb-pcCPG also showed photochromic behaviour based on DTE ring-opening/closing (Fig. S21†). Yellow coloured Tb-pcCPG-O can be converted to blue Tb-pcCPG-C by UV-irradiation which can be reverted by visible light treatment. The PXRD pattern and FT-IR spectrum of Tb-pcCPG-O was found to be similar to those of the Eu-pcCPG-O (Fig. S19 and S20†). This indicates the presence of π–π interaction and H-bonding in the self-assembly of Tb-pcCPG-O, similar to the Eu-pcCPG-O. FESEM and TEM analyses of Tb-pcCPG-O showed the interconnected spherical morphology similar to the Eu-pcCPG-O (Fig. S22†). The elemental mapping of Tb-pcCPG-O showed uniform distribution of Tb^{3+} (Fig. S23†), whereas EDAX analysis revealed the presence of 11.08 wt% Tb in Tb-pcCPG-O (Fig. S23†). Notably, upon excitation at 310 nm, Tb-pcCPG-O displayed four Tb^{3+} centred emission peaks with maxima at 490 ($^5D_4$–$^7F_3$), 546 ($^5D_4$–$^7F_4$), 587 ($^5D_4$–$^7F_5$), and 623 ($^5D_4$–$^7F_6$) nm (Fig. 5a). The highest intensity peak among all four bands was observed at 546 nm corresponding to $^5D_4$–$^7F_4$ transition and responsible for the green emission of Tb-pcCPG-O.[56] Importantly, emission of Tb-pcCPG-O has a poor overlap with the absorption of the closed form of Tb-pcCPG-C, and therefore, an effective pcFRET

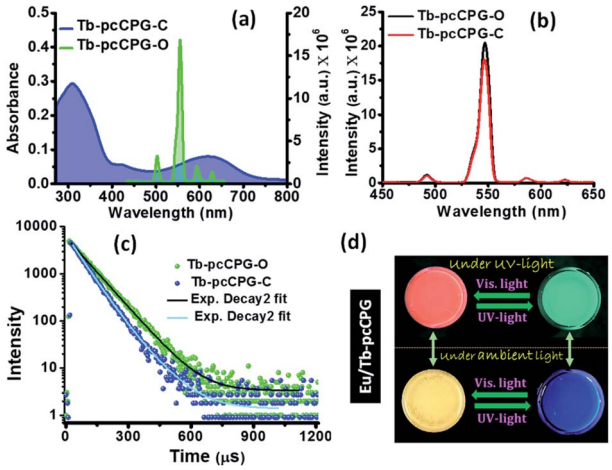

Fig. 5 (a) Absorption spectrum of Tb-pcCPG-C (blue) and emission spectrum of Tb-pcCPG-O (green). (b) Emission spectra of Tb-pcCPG-O and Tb-pcCPG-C. (c) Time resolved photoluminescence decay profiles for Tb-pcCPG-O and Tb-pcCPG-C (λ_{ex} = 310 nm and λ_{em} = 546 nm). (d) Images of colour change for the mixed gel system (Eu/Tb-pcCPG) under UV and visible light.

was not observed (Fig. 5a). This was further evident as UV irradiation for 60 seconds on the Tb-pcCPG-O showed insignificant emission quenching in Tb-pcCPG-C and the bright green emission remained intact (Fig. 5b and S21a†). Moreover, the quantum yield of Tb-pcCPG before and after UV irradiation remained similar and was found to be 23.4% and 21.1%, respectively. The decay profile for the excited-state lifetime for the photoisomers of Tb-pcCPG was found to be biexponential, similar to that of the Eu-pcCPG. The lifetime value for Tb-pcCPG-O and Tb-pcCPG-C was calculated to be 87.0 μs and 82.7 μs, respectively, indicating inefficient pcFRET (energy transfer efficiency = 4.94%) in this case (Fig. 5c, Table S3†).

Furthermore, as mentioned above, the emission of Tb-pcCPG was not photo-switchable and remained intact in the presence and absence of UV-light. Therefore, we were interested in examining the emission outcome of a gel based on a mixed metal (Eu/Tb-pcCPG) system. The optimized gel of Eu : Tb (7 : 3 ratio) pcCPG-O was obtained upon heating at 80 °C (see the details in the ESI†). The Eu/Tb-pcCPG-O excited at 310 nm showed distinct peaks for both Eu^{3+} and Tb^{3+} (Fig. S24†). However, bright red emission for Eu/Tb-pcCPG-O was detected by the naked eye due to the higher concentration of Eu^{3+} ions (Fig. 5d). Interestingly, owing to the photo-switchable emission properties of Eu-pcCPG, UV-irradiation on the mixed gel (Eu/Tb-pcCPG) system for 40 seconds resulted in quenching of red emission and yielded bright green emission that can be assigned to Tb-pcCPG-C. Notably, this green emissive mixed-gel was blue in colour under daylight. The emission spectrum recorded after UV-irradiation on the mixed gel sample showed Tb^{3+}-centred emission. Thus, emission of a mixed lanthanide-based gel has been modulated reversibly upon light treatment, which is yet to be explored for the CPG system. Therefore, photo-modulated reversible colour changes, yellow ↔ red ↔ green ↔ blue ↔ yellow, can be achieved for Eu/Tb-pcCPG upon shining suitable light which is unprecedented in CPG systems (Fig. 5d). These photo-modulated emission and visible colour changes of mixed Eu/Tb-pcCPG can be employed for signalling applications.[50,54]

Conclusions

The present study demonstrated the design and synthesis of a DTE based LWMG and preparation of a highly processable photochromic organogel. Further, the LWMG has been exploited for developing Eu^{3+} and Tb^{3+} based photochromic coordination polymer gels (Eu-pcCPG and Tb-pcCPG). The Eu-pcCPG has shown reversible morphology transformation from spheres to fibres and *vice versa* upon treating with UV and visible light, respectively. The Eu-pcCPG showed excellent photo-switchable emission and displayed impressive pcFRET with an energy transfer (ET) efficiency of 94.79%. The importance of spectral overlap for pcFRET in Eu-pcCPG has also been justified by Tb-pcCPG. Further, a mixed metal Eu^{3+}/Tb^{3+} pcCPG (in 7 : 3 ratio) showed excellent reversible photo-modulated luminescence as well as photochromism that can be utilized for signalling applications. Owing to the high processability, Eu-pcCPG has been utilized as smart ink for secret writing on ordinary paper. Interestingly, the written information appeared only for a few seconds under UV-light and therefore it could be employed for encrypting confidential information. The photo-switchable photophysical properties combined with the high processability of such materials could open exciting opportunities towards developing smart materials for optoelectronics and microscopy applications.

Conflicts of interest

There are no conflicts to declare.

Acknowledgements

PV acknowledges the Council of Scientific and Industrial Research (CSIR), Govt. of India, for the fellowship. TKM acknowledges the SERB, Dept. of Science and Technology (DST), Govt. of India for financial support (project no. CRG/2019/005951). The authors are thankful to Prof. R. Ganapathy and Mr M. Chaudhary for their help with rheology measurements.

Notes and references

1 J. H. Jung, J. H. Lee, J. R. Silverman and G. John, *Chem. Soc. Rev.*, 2013, **42**, 924–936.
2 P. Sutar and T. K. Maji, *Chem. Commun.*, 2016, **52**, 8055–8074.
3 A. J. Savyasachi, O. Kotova, S. Shanmugaraju, S. J. Bradberry, G. M. O. Maille and T. Gunnlaugsson, *Chem*, 2017, **3**, 764–811.
4 M. O. M. Piepenbrock, G. O. Lloyd, N. Clarke and J. W. Steed, *Chem. Rev.*, 2010, **110**, 1960–2004.
5 S. C. Wei, M. Pan, K. Li, S. Wang, J. Zhang and C. Y. Su, *Adv. Mater.*, 2013, **26**, 2072–2077.

6 A. E. Cabrera, A. Rapakousiou, M. P. Bello, G. Molnar, L. Salmon and A. Bousseksou, *Coord. Chem. Rev.*, 2020, **419**, 213396–213419.
7 J. C. H. Chan, W. H. Lam, H. L. Wong, W. T. Wong and V. W. W. Yam, *Angew. Chem., Int. Ed.*, 2013, **52**, 11504–11508.
8 K. Lalitha, Y. S. Prasad, V. Sridharan, C. U. Maheswari, G. John and S. Nagarajan, *RSC Adv.*, 2015, **5**, 77589–77594.
9 P. Sutar, V. M. Suresh, K. Jayaramulu, A. Hazra and T. K. Maji, *Nat. Commun.*, 2018, **9**, 3587–3598.
10 D. Okada, Z. H. Lin, J. S. Huang, O. Oki, M. Morimoto, X. Liu, T. Minari, S. Ishii, T. Nagao, M. Irie and Y. Yamamoto, *Mater. Horiz.*, 2020, **7**, 1801–1808.
11 D. Pinkowicz, M. Ren, L. M. Zheng, S. Sato, M. Hasegawa, M. Morimoto, M. Irie, B. K. Breedlove, G. Cosquer, K. Katoh and M. Yamashita, *Chem.–Eur. J.*, 2014, **20**, 12502–12513.
12 Y. Hamo, M. Lahav and M. E. V. D. Boom, *Angew. Chem., Int. Ed.*, 2020, **59**, 2612–2617.
13 P. Sutar and T. K. Maji, *Dalton Trans.*, 2020, **49**, 7658–7672.
14 M. C. Heffern, L. M. Matosziuk and T. J. Meade, *Chem. Rev.*, 2014, **114**, 4496–4539.
15 A. D. Aleo, F. Pointillart, L. Ouahab, C. Andraud and O. Maury, *Coord. Chem. Rev.*, 2012, **256**, 1604–1620.
16 H. Dong, L. D. Sun and C. H. Yan, *Nanoscale*, 2013, **5**, 5703–5714.
17 H. B. Cheng, H. Y. Zhang and Y. Liu, *J. Am. Chem. Soc.*, 2013, **135**, 10190–10193.
18 J. Boixel, V. Guerchais, H. L. Bozec, D. Jacquemin, A. Amar, A. Boucekkine, A. Colombo, C. Dragonetti, D. Marinotto, D. Roberto, S. Righetto and R. D. Angelis, *J. Am. Chem. Soc.*, 2014, **136**, 5367–5375.
19 G. Naren, C. W. Hsu, S. Li, M. Morimoto, S. Tang, J. Hernando, G. Guirado, M. Irie, F. M. Raymo, H. Sunden and J. Andreasson, *Nat. Commun.*, 2019, **10**, 3996–4002.
20 S. Pandya, J. Yu and D. Parker, *Dalton Trans.*, 2006, 2757–2766.
21 C. L. Wong, M. Ng, E. Y. H. Hong, Y. C. Wong, M. Y. Chan and V. W. W. Yam, *J. Am. Chem. Soc.*, 2020, **142**, 12193–12206.
22 B. Oruganti, P. P. Kalapos, V. Bhargav, G. London and B. Durbeej, *J. Am. Chem. Soc.*, 2020, **142**, 13941–13953.
23 C. Li, K. Xiong, Y. Chen, C. Fan, Y. L. Wang, H. Ye and M. Q. Zhu, *ACS Appl. Mater. Interfaces*, 2020, **12**, 27651–27662.
24 D. Dulic, T. Kudernac, A. Puzys, B. L. Feringa and B. J. v. Wees, *Adv. Mater.*, 2007, **19**, 2898–2902.
25 S. E. Cakmak, D. A. Leigh, C. T. McTernan and A. L. Nussbaumer, *Chem. Rev.*, 2015, **115**, 10081–10206.
26 B. Qin, H. Chen, H. Liang, L. Fu, X. Liu, X. Qiu, S. Liu, R. Song and Z. Tang, *J. Am. Chem. Soc.*, 2010, **132**, 2886–2888.
27 H. Zheng, B. Ju, X. Wang, W. Wang, M. Li, Z. Tang, S. X. Zhang and Y. Xu, *Adv. Opt. Mater.*, 2018, **6**, 1801246–1801253.
28 S. Bhattacharya, M. Maity, A. Chaudhury, M. L. Saha, P. J. Stang and P. S. Mukherjee, *Inorg. Chem.*, 2020, **59**, 2083–2091.
29 R. Saha and P. S. Mukherjee, *Dalton Trans.*, 2020, **49**, 1716–1720.
30 P. Sutar and T. K. Maji, *Inorg. Chem.*, 2017, **56**, 9417–9425.
31 Q. Luo, H. Cheng and H. Tian, *Polym. Chem.*, 2011, **2**, 2435–2443.
32 M. M. Russew and S. Hecht, *Adv. Mater.*, 2010, **22**, 3348–3360.
33 C. C. Ko and V. W. W. Yam, *J. Mater. Chem.*, 2010, **20**, 2063–2070.
34 R. Klajn, J. F. Stoddart and B. A. Grzybowski, *Chem. Soc. Rev.*, 2010, **39**, 2203–2237.
35 Y. Gu, E. A. Alt, H. Wang, X. Li, A. P. Willard and J. A. Johnson, *Nature*, 2018, **560**, 65–69.
36 K. Uno, M. L. Bossi, V. N. Belov, M. Irie and S. W. Hell, *Chem. Commun.*, 2020, **56**, 2198–2201.
37 Z. Zhang, W. Wang, P. Jin, J. Xue, L. Sun, J. Huang, J. Zhang and H. Tian, *Nat. Commun.*, 2019, **10**, 4232–4240.
38 K. Shibata, K. Muto, S. Kobatake and M. Irie, *J. Phys. Chem. A*, 2002, **106**, 209–214.
39 A. Singh, P. Verma, S. Laha, D. Samanta, S. Roy and T. K. Maji, *ACS Appl. Mater. Interfaces*, 2020, **12**, 20991–20997.
40 G. M. Peters and J. D. Tovar, *J. Am. Chem. Soc.*, 2019, **141**, 3146–3152.
41 C. P. Harvey and J. D. Tovar, *Polym. Chem.*, 2011, **2**, 2699–2706.
42 D. Samanta, A. Singh, P. Verma, S. Bhattacharyya, S. Roy and T. K. Maji, *J. Org. Chem.*, 2019, **84**, 10946–10952.
43 G. Li, S. Zhao, Y. Zhang and Z. Tang, *Adv. Mater.*, 2018, **30**, 1800702–1800743.
44 Y. Li, J. Liu, Z. Wang, J. Jin, Y. Liu, C. Chen and Z. Tang, *Adv. Mater.*, 2020, **32**, 1907718–1907727.
45 D. Samanta, S. Roy, R. Sasmal, N. D. Saha, K. R. Pradeep, R. Viswanatha, S. S. Agasti and T. K. Maji, *Angew. Chem., Int. Ed.*, 2019, **58**, 5008–5012.
46 J. Zhang and H. Tian, *Adv. Opt. Mater.*, 2018, 1701278–1701307.
47 Z. Li, G. Wang, Y. Ye, B. Li, H. Li and B. Chen, *Angew. Chem., Int. Ed.*, 2019, **58**, 18025–18031.
48 J.-F. Mei, Z. P. Lv, J. C. Lai, X. Y. Jia, C. H. Li, J. L. Zuo and X. Z. You, *Dalton Trans.*, 2016, **45**, 5451–5454.
49 X. He, L. Norel, Y. M. Hervault, R. Metivier, A. D. Aleo, O. Maury and S. Rigaut, *Inorg. Chem.*, 2016, **55**, 12635–12643.
50 H. Zhao, X. Qin, L. Zhao, S. Dong, L. Gu, W. Sun, D. Wang and Y. Zheng, *ACS Appl. Mater. Interfaces*, 2020, **12**, 8952–8960.
51 B. Z. Wang, Y. Ma, R. Zhang, A. Peng, Q. Liao, Z. Cao, H. Fu and J. Yao, *Adv. Mater.*, 2009, **21**, 1737–1741.
52 T. Nakagawa, Y. Hasegawa and T. Kawai, *Chem. Commun.*, 2009, 5630–5632.
53 M. Yano, K. Matsuhira, M. Tatsumi, Y. Kashiwagi, M. Nakamoto, M. Oyama, K. Ohkubo, S. Fukuzumi, H. Misakif and H. Tsukubef, *Chem. Commun.*, 2012, **48**, 4082–4084.
54 Z. Li, H. Chen, B. Li, Y. Xie, X. Gong, X. Liu, H. Li and Y. Zhao, *Adv. Sci.*, 2019, **6**, 1901529–1901536.

55 C. W. Hsu, C. Sauvee, H. Sunden and J. Andreasson, *Chem. Sci.*, 2018, **9**, 8019–8023.
56 M. M. Calvo, O. Kotova, M. E. Mobius, A. P. Bell, T. McCabe, J. J. Boland and T. Gunnlaugsson, *J. Am. Chem. Soc.*, 2015, **137**, 1983–1992.
57 J. R. Sorg, T. Schneider, L. Wohlfarth, T. C. Schafer, A. Sedykh and K. M. Buschbaum, *Dalton Trans.*, 2020, **49**, 4904–4913.
58 H. Song, X. Liu, B. Wang, Z. Tang and S. Lu, *Sci. Bull.*, 2019, **64**, 1788–1794.
59 Y. Cui, Y. Yue, G. Qian and B. Chen, *Chem. Rev.*, 2012, **112**, 1126–1162.
60 W. Jeong, M. I. Khazi, D. H. Park, Y. S. Jung and J. M. Kim, *Adv. Funct. Mater.*, 2016, **26**, 5230–5238.
61 H. Sato, T. Matsui, Z. Chen, J. Pirillo, Y. Hijikata and T. Aida, *J. Am. Chem. Soc.*, 2020, **142**, 14069–14073.
62 P. Sutar and T. K. Maji, *Chem. Commun.*, 2016, **52**, 13136–13139.
63 K. Higashiguchi, G. Taira, J. i. Kitai, T. Hirose and K. Matsuda, *J. Am. Chem. Soc.*, 2015, **137**, 2722–2729.
64 J. J. D. d. Jong, W. R. Browne, M. Walko, L. N. Lucas, L. J. Barrett, J. J. McGarvey, J. H. v. Escha and B. L. Feringa, *Org. Biomol. Chem.*, 2006, **4**, 2387–2392.
65 M. C. Mantero, L. Oggioni, G. Pariani, F. Ortica, S. Tosi, M. Canepa, C. Bertarelli, M. Tommasini and A. Bianco, *RSC Adv.*, 2020, **10**, 26177–26187.
66 P. Sutar, V. M. Suresh and T. K. Maji, *Chem. Commun.*, 2015, **51**, 9876–9879.
67 A. Singh and G. Ramanathan, *J. Lumin.*, 2017, **182**, 220–225.
68 S. Wintzheimer, J. Reichstein, S. Wenderoth, S. Hasselmann, M. Oppmann, M. T. Seuffert, K. M. Buschbaum and K. Mandel, *Adv. Funct. Mater.*, 2019, **29**, 1901193–1901204.
69 C. E. Rowland, J. B. Delehanty, C. L. Dwyer and I. L. Medintz, *Mater. Today*, 2017, **20**, 131–141.
70 P. Zhang, Y. Wang, H. Liu and Y. Chen, *J. Mater. Chem.*, 2011, **21**, 18462–18466.
71 N. Kumar, G. Sandi, M. Kaminski, A. Bobadilla, C. Mertz and J. M. Seminario, *J. Phys. Chem. C*, 2015, **119**, 12037–12046.